Energy efficiency maximization in a wireless powered IoT sensor network for water quality monitoring

Segun O. Olatinwo [a,*] and Trudi-H. Joubert [a]

[a] Department of Electrical, Electronic and Computer Engineering, University of Pretoria, Pretoria 0001, South Africa

***** Correspondence email: segunlatinwo@gmail.com; trudi.joubert@up.ac.za

ABSTRACT

This study presents novel approaches to the allocation of resources in Internet-of-Things sensor network (IoTSN) systems applied to water-quality monitoring for optimal and more sustainable utilization of resources. To tackle the long-standing energy scarcity issue that currently plagues sensor network (SN) systems, energy harvesting is explored and exploited to maximize its untapped potential to develop a successive wireless power sensor network (WPSN) system embedded with a scheduling algorithm, and operate as a non-orthogonal multiple access (NOMA) system. Similarly, quality of service parameters are crucial design considerations for network efficiency, and energy efficiency (EE) is considered here. Consequently, an EE optimization problem is formulated for the successive WPSN system and solved by exploiting the problem structure and through a meta-heuristic algorithm. The new system is validated through the numerical simulation results presented in this work by thoroughly analyzing, evaluating and comparing the proposed meta-heuristic based WPSN system with the baseline state-of-the-art WPSN systems that combined a meta-heuristic algorithm, two additional meta-heuristic algorithms including genetic algorithm (GA) and ant-colony optimization (ACO) algorithm as well as a non-meta-heuristic algorithm – specifically an iterative based Dinkelbach algorithm. The experimental outcomes show that the proposed system significantly outperforms the contemporary WPSN systems in terms of EE performance gains.

Keywords: Water quality, wirelessly powered network, RF energy harvesting, internet-of-things, ant-colony optimization, particle swarm optimization, non-orthogonal multiple access, energy efficiency, green communication.

1. Introduction

Today, water-related illnesses are rampant. This can be attributed to the issue of not having access to safe water [1] – [4]. Safe water simply refers to clean water and is a vital substance for humans and animals [1]. In essence, their survival depends on clean water. Therefore, ensuring the cleanliness of water at all times is essential as the ingestion of poor quality water is highly harmful to the health as a result of the presence of micro-organisms and metal-ions [2], [3] - which is mostly influenced by anthropogenic activities. This consequently necessitates the desire for cost-effective and reliable systems such as wireless sensor networks (WSNs) to overcome the shortcomings of the traditional laboratory-based water quality analysis systems. In WSNs, the Internet-of-Things (IoT) has emerged as a central technology that drives the data communication process of WSN systems through the connection of the network sensor nodes to the Internet [5] – [7]. The amalgamation of the IoT and WSNs forming the Internet-of-Things sensor network (IoTSN) has brought new opportunities to the environmental monitoring domain such as remote water quality monitoring (WQM).

The usage of IoTSN in WQM helps to detect possible water contamination in a timely manner, which assists in guarding against the distribution of polluted water. Unfortunately, IoTSNs in WQM suffer from inherent network energy problems, including energy scarcity and high energy expenditure [8]. To address the scarceness of energy, wireless energy transfer (WET) techniques that exploit radio frequency (RF) signal to transfer RF energy has recently emerged for powering IoTSNs. This line of research is referred to as wireless power sensor networks (WPSNs). Note that energy is a very scarce resource that needs to be efficiently utilized since WSNs are energy constrained communication networks, giving scope for the optimization of energy efficiency (EE) as well as throughput rate in WPSNs. Recently, there have been some research attempts on throughput and energy utilization optimization, for example, [4], [8], [9] have considered the throughput and energy utilization optimization of the WPSN systems by developing efficient optimization solutions that jointly optimizes the constrained resources like time resource allocation for harvesting RF energy and transmitting signals (or data bits). The idea of maximizing the throughput performance of WPSN communication networks is an essential design objective to develop efficient networks that can reliably communicates their data bits. Currently, there are a few works in the literature that focused on the maximization of WPSNs' performance in terms of energy efficiency, and examples of such works are references [10] - [15]. In [10], the authors considered the EE maximization of a mobile WSN system where an ambient RF technique was used as power source to increase the lifetime of the system's relay nodes and cluster

nodes. To enable the relays and the clusters to receive RF signals from their environment, as well as empower the relay nodes to forward their data packets through the neighboring relays in a multi-hop manner to a specific cluster node where a mobile collector receives the aggregated data, a simultaneous wireless information power transfer (SWIPT) model was employed. RF energy harvesting (EH) from ambient sources may not be efficient as it is not deterministic and controllable, hence, it may be difficult to guarantee the reliability of such systems. Also, the use of the SWIPT model is costly in practice and may suffer from interference problem, and unfairness problem if the received RF signals are not efficiently allocated for EH and signal processing purposes. To deal with these problems, this work considered RF EH from dedicated power stations and signal processing using the wireless information power transfer (WIPT) model, which is easy to implement and cost-effective in practice. Also, [11] has considered the optimization of the EE of a WSN system and the exploitation of the SWIPT model for RF EH and information processing purposes. Unlike [11], the WIPT model is considered in this work to circumvent unfairness and interference problems. References [12] – [15] have considered a single dedicated RF power source (DPS) for powering their WPSN systems with a WIPT model. In contrast to [12] - [15], multiple DPSs are considered in this work. In the prior works a hybrid RF power source-sink node is considered, which implies that their DPS node and the sink node are co-located. Because of the co-habitation of the nodes, an inherent problem named doubly near far, is encountered by the networks. To deal with aforementioned problem so as to improve the harvested energy as well as minimize the time spent for charging the sensors' in-built batteries, multiple dedicated DPSs are considered. One of the DPSs performs a co-located function, and this node is referred to as a hybrid RF power source-sink node (HPSSN). Note that only the HPSSN can both broadcast energy to the water quality sensors (WQSs), as well as receive water quality data from the scheduled WQSs for information transmission, while the rest of the DPSs can only broadcast energy to the WQSs. Furthermore, in this work a new data communication scheduling scheme is considered to consecutively classify the WQSs based on data communication priority into two distinct groups and cycles, namely group 1 and group 2 in the uplink (UL), such that the newly proposed successive WPSN system schedules the WQSs in group 1 to transmit their signals during cycle 1, while the WQSs in the group 2 are enabled in cycle 2 for data communication, in a non-orthogonal multiple access (NOMA) protocol. One of the key agendas of this contribution is to optimize the energy expenditure of the overall network to improve the energy efficiency of the proposed system. NOMA is a 5G-supported protocol that provides multiple access to sensor nodes in the power domain by multiplexing the sensor nodes on the same resources through the exploitation of a superposition coding strategy implemented at the transmitter-side of the sensor nodes and an advanced receiver, that is embedded with a successive interference cancellation (SIC) technique [16]. The potential of a NOMA protocol has made it a promising protocol for enhancing the spectral efficiency and energy efficiency of communication systems like wireless powered IoT sensor networks [17], [18]. Consequently, in this work, the development of a successive WPSN system for WQM application use-case is considered. A crucial aspect of this study is to formulate strategies that can efficiently control the usage of resources in the new WPSN system. The key contributions made by this study are five-fold and are highlighted by the following points:

- The development of a successive WPSN is proposed to prioritize the operation of WQSs in the UL. For energy efficient communication in WPSN, all the WQSs may not necessarily transmit information during the UL stage; this is an important strategy in WPSN.
- The integration of a non-orthogonal multiple access (NOMA) scheme into a successive WPSN for communication and resources (such as power and time) allocation purposes.
- The optimization of the power and time resources through the exploitation of the adopted NOMA scheme to improve the performance of the system in term EE.
- Formulation of a data-related EE maximization problem.
- Design of a meta-heuristic solution for optimally solving the EE problem.
- For the first time, this study presents the formulation of the EH model for multiple power stations in a NOMA system that has EE maximization for greener communication.

To our best knowledge, no study has considered a successive WPSN solution model in literature on a system for a WQM application scenario. The rest of this study is divided into sections with Section 2 presenting the model of the new WPSN system; Section 3 discussing mathematical models on the system wireless channel, the EH and data transmission algorithms, and energy consumption; in Section 4 details are provided on the formulation of the new system's EE as an optimization problem; the proposed solution to the optimization problem is detailed in Section 5; in Section 6 the discussion of the simulation results takes place to validate the new WPSN system; and finally the study is concluded in Section 7.

2. Proposed system architecture

This study presents a new system architecture that is composed of a WPSN containing j successive sensors that are classified into two distinct groups namely group 1 and group 2 as shown in Fig. 1 based on their information transmission scheduling priority which is based on a successive data communication scheduling method such that group 1 that contains i sensors, $j \in i = \{i_1, i_2, \dots, I\}$ is enabled for information transmission in first cycle at the UL phase, while group 2 that contains q sensors, $j \in q = \{q_1, q, \dots, Q\}$ is scheduled to transmit water quality information at the second cycle of the UL phase. Consequently, groups 1 and 2 sensors are enabled for data communication at the UL at different times. Because of simultaneous transmission of the water quality information by each group of sensors at the scheduled period to the sink node, indicative of many-to-one data communication, a SIC mechanism is considered at the receiver as a data-

congestion control measure to separate each of the sensors that concurrently transmits their data to the sink node. Similarly as done in [19], this mechanism facilitates the sequential decoding of the data that are simultaneously broadcast by the sensors.

The employed sensor nodes are WQSs that measure key microbiological and chemical properties used in WQM, such as E. coli concentration and pH, at a water-processing station. Note that all the WQSs may not necessarily transmit information during the UL stage, thus, only one group of sensors is enabled in a cycle. Both the groups 1 and 2 WQS nodes are powered by the DPSs, with an index of g. One particular g is represented using g_1 (for the HPSSN), that performs the functions of the hybrid power source and sink node. Each DPS is connected to a power source, and as had been assumed in the work of [13], [20], and [21], has complete channel state information (CSI) knowledge. According to the CSI knowledge, the DPSs g initially transmits continuous RF power signals to all nodes simultaneously for a duration of τ with a power of $P_{A,g}$. As clearly described in the experiments carried out in [22], it is important to note that the charging time needed to charge the groups 1 and 2 nodes i and q batteries is always within seconds.

The scheduled nodes for information transmission in the group expend the RF energy harvested in a specific cycle to communicate their independent water-quality-related data to the sink node based on a transmission power defined by p_i for $i = \{i_1, i_2, \dots, I\}$ and p_q for $q = \{q_1, q, \dots, Q\}$ respectively, and a duration of transmission of β. The received water-quality-related data by the HPSSN may be advantageously utilized by the local users to gain a timely insight into the quality of the concerned water body. The details of received data could be seamlessly routed to remote locations through the usage of communication networks with internet capabilities. These provisions make it possible to efficiently track any possible changes in the quality of water as well as timeously detect if there are microbes and chemical manifestations - all these are essential for proactive decision making and management purposes in the event of contamination. Both group 1 and 2 nodes are configured in a single-hop manner, such that each WQS node sends its independent information signal to the sink node at a scheduled cycle. The WQSs, indexed by i and q, and the DPSs have a single omnidirectional antenna, and they are operate based on a NOMA model over the same unlicensed ISM frequency band. The in-built batteries of the WQSs is assumed to possibly contain reserved energy from the previous transmission block, and the quantity of the initial (or left-over) energy stored is represented as e_i and e_q for WQSs i and q, respectively. Such energy is useful to support the transmission of data bits at the UL stage. As in [23] and [24], it is assumed in this work that the energy consumed for setting up the initial network is independent of the energy harvested as it is drawn from a battery which is not necessarily powered by energy harvesting, and consequently the initial energy is assumed to be 0.

The sensor positioning is carried out using a random approach, in contrast to a pre-determined deployment approach, to cater for the need of eventually placing the sensors at strategic points for optimal monitoring of the parameters of a water body site as described in Fig. 1. Consequently, this prompted the provision of a synthetic apparatus that gives room for the flow of the water body to be devised as similarly done in [8] and [25]. The devised provision creates a suitable platform to ease the deployment process of the WQSs and also facilitates the realization of the needed constant water flow. The purpose of the successive concept is an attempt to maximize the energy efficiency of the proposed system. To realize this, the system decides the enablement of a specific group of WQSs for data transmission and the one that is not expected to include in data transmission process at a particular time. Note that the proposed WPSN model integrates a controller that has a global knowledge of the network resources, nodes including WQSs i and q in groups 1 and 2, respectively, as well as a scheduler to enable either group 1 or group 2 for data communication in a cycle based on a pre-defined priority. It is important to point out that the controller updates its information about the network sensors for synchronization purposes, while the energy spent by the sensors for updating is drawn from the separate batteries. As in [4], [8], [20], this work has adopted the concept that the operation of the controller in switching on and off DPSs at an allocated time guards against any form of destructive interference due to the emission of RF energy, as well as updating the knowledge of the network nodes at the controller. Since the DPSs are specifically deployed in strategic locations, the knowledge of their locations is acquired by the controller during the configuration process of the DPSs, which is similar to the case of the base station controller and base stations configuration in a cellular network system [20]. Similarly, it is reasonable for the controller to know the sensor nodes in the network since they could make themselves aware to the controller during their first data transmission piggy-backed registration message to the controller, including their positions. Based on the described knowledge, it is practical that the controller perfectly knows the energy status of the sensors as the energy received from the DPSs by each sensor during a transmission block may be reported through each data transmission piggy-backed process. This approach helps to keep the status of sensors updated at the controller while incurring no signaling overhead.

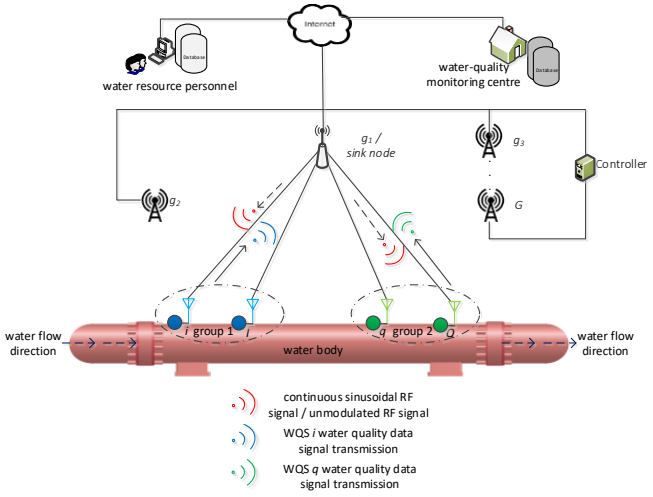

Fig. 1. Architecture of the proposed successive WPSN system for water-quality monitoring

3. Mathematical models

3.1. *Wireless channel model*

The new WPSN communication network assumes a static environment, therefore, the fading model adopted for modelling the DL channel gain from the DPSs g to the WQSs i and q, and vice-versa for UL channel gain, is a quasi-static block. The model is applied to form the channel power gain between the DPSs g, and a WQSs i and q. The channel between the g and i as well as q in the DL, including the opposite channel between i and g and also q and g in the UL, are denoted by the complex channel gains $\tilde{b}_{g,i}$ and $\tilde{b}_{g,q}$, and $\tilde{a}_{g,i}$ and $\tilde{a}_{g,q}$ respectively. The directional channel gains that results from the complex channel gains are now $b_{g,i} = \left|\tilde{b}_{g,i}\right|^2$ and $a_{g,i} = \left|\tilde{a}_{g,i}\right|^2$ and $b_{g,q} = \left|\tilde{b}_{g,q}\right|^2$ and $a_{g,q} = \left|\tilde{a}_{g,q}\right|^2$ for group 1 and 2, respectively. As in [13], [20], [21], the DL channel links, i.e., the $b_{g,i}$'s and $b_{g,q}$'s as well as the UL channel links, i.e., the $a_{g,i}$'s and $a_{g,q}$'s CSI are assumed to be perfectly known at the HPSSN, and based on the CSI knowledge at the transmitter side of the HPSSN including the DPSs g, transmission of energy the WQSs i and q is achieved adaptively based on the channel states and the allocated duration transmission period. In the proposed NOMA scheme, the transmission duration τ is intended for energy transmission to all the WQSs i and q simultaneously, while the transmission duration β is dedicated to information transmission by one of the groups per cycle.

3.2. *Energy harvesting and data transmission models*

The proposed NOMA scheme is developed to operate as a half-duplex protocol to effectively cater for harvesting and data communication purposes. For the harvesting of energy operation, a duration τ defined by $0 \leq \tau \leq 1$ is allocated to the DPSs to concurrently broadcast energy to the WQSs i and q at the same time in the DL, as well, a duration of $0 \leq \beta \leq 1$ is allocated for the transmission of information and is assigned to either $\beta \in \{i_1, i_2, \dots, I\}$ or $\beta \in \{q_1, q, \dots, Q\}$ to individually communicate their information at a scheduled period to the sink node g_1 over either channel $a_{1,i}$ or $a_{1,q}$ in the UL. As a result of the concurrent transmissions at the UL by either group 1 or group 2 at the scheduled period, we consider a successive interference cancellation technique at the receiver to sequentially decode each of WQSs $\{i_1, i_2, \dots, I\}$ and $\{q_1, q, \dots, Q\}$ data signal and distinguish the data signals sent by differentiating the WQS nodes. Therefore, the total available EH duration as well data transmission duration is provided in (1) as:

$$\tau + \beta \leq 1 \quad \in \text{group } 1 \cup \text{group } 2 \tag{1}$$

The power received at sensor i from all the DPSs is modeled in (2) as:

$$x_{g,i} = \sqrt{b_{g,i}} x_{A,g} + z_i, \forall_i \tag{2}$$

In (2), $x_{g,i}$ stands for the received power signal containing the RF energy from the DPSs, while z_i stands for WQS $i's$ background noise power. $x_{A,g}$ stands for the complex random signal arbitrarily transmitted by a DPS and fulfils $\mathbb{E}\left[\left|x_{A,g}\right|^2\right] = P_{A,g}$. $P_{A,g}$ stands for the power of transmission of a DPS, and is large enough that the WQS $i's$ background noise power may be assumed negligible. As a result, the energy that WQSs i could harvest from all the DPSs at the DL is formulated in (3) as:

$$E_i = \eta_i \sum_{g=1}^{G} P_{A,g}\, b_{g,i} \tau + e_i, \forall_i \quad \text{(J)} \tag{3}$$

In (3), η_i represents WQS $i's$ energy conversion efficiency, and for the purpose of simplicity the same efficiency is assumed for all WQSs. In consequence, equation (3) transforms to (4):

$$E_i = \eta \sum_{g=1}^{G} P_{A,g}\, b_{g,i} \tau + e_i, \forall_i \tag{4}$$

By adopting the Shannon Hartley information theory, the number of data bits that may be transmitted by the WQS i in group 1 is modelled in (5) as:

$$r_i(\boldsymbol{\mu}, p_i) = \beta W \log_2\left(1 + \frac{a_{1,i}\, p_i}{\sum_{d=i+1}^{I} a_{1,d}\, p_d + \sigma^2}\right), \quad \forall_i \in \{i_1, i_2, \dots, I\} \tag{5}$$

In (5), W stands for the system's bandwidth, $a_{1,i}$ models the UL channel-link employed by the group 1 WQS $i's$ in to individually broadcast their water-quality-related data signal to sink node g_1, p_i stands for WQS $i's$ transmission power, and the noise power the sink node received is defined by σ^2. The time resource allocation as well as the power resource allocation are formulated as vector $\boldsymbol{\mu} \triangleq [\tau, \beta]^T$ and vector $p_i \triangleq [p_1, p_2, \dots, p_I]^T$, respectively. It is important to ensure that each WQS i in group 1 meets its minimum quality-of-service (QoS) rate for reliable data transmission, hence, the minimum required QoS rate set for the WQS i is denoted by R_i, and is formulated in (6) as:

$$r_i(\boldsymbol{\mu}, p_i) \geq R_i, \forall_i \tag{6}$$

In the subsequent achievable data transmission expression, $\frac{a_{1,i}}{\sigma^2}$ is represented by $\bar{a}_{1,i}$. From (5), the sum of the number of data bits that the WQSs i in group 1 could transmit is given in (7) as:

$$R_{sum}(\boldsymbol{\mu}, p_i) = \sum_{i=1}^{I} r_i(\boldsymbol{\mu}, p_i), \forall_i \tag{7}$$

Also, since the operation of the WQS nodes is based on a successive method then the details of the WQSs in group 2 are provided as follows:

$$R_{sum}(\boldsymbol{\mu}, p_i) = \beta W \log_2\left(\sum_{i=1}^{I} \bar{a}_{1,i}\, p_i + 1\right), \forall_i \tag{8}$$

The power received at sensor q from all the DPSs is modeled in (9) as:

$$x_{g,q} = \sqrt{b_{g,q}} x_{A,g} + z_q, \forall_q \tag{9}$$

The harvested energy by WQS q at the DL during duration τ from all the DPSs is modelled in (10) as:

$$E_q = \eta \sum_{g=1}^{G} P_{A,g}\, b_{g,q} \tau + e_q, \forall_q \quad \text{(J)} \tag{10}$$

The number of data bits that WQS q in group 2 could transmit is modelled in (11) as:

$$r_q(\boldsymbol{\mu}, p_q) = \beta W \log_2\left(1 + \frac{a_{1,q}\, p_q}{\sum_{d=q+1}^{Q} a_{1,d}\, p_d + \sigma^2}\right), \quad \forall_q \in \{i_q,\ i_q, \dots,\ Q\} \tag{11}$$

where W is the system's bandwidth, $a_{1,q}$ denotes the UL channel model for WQS q in group 2 to communicate their independently generated data to g_1, using a transmission power defined as p_q as well as duration β. Thus, the power resource and the time allocation vectors are $p_q \triangleq [p_1, p_2, \dots, p_I]^T$ and vector $\boldsymbol{\mu} \triangleq [\tau, \beta]^T$, respectively. To satisfy the minimum data bits QoS requirements of WQS q for reliable data transmission, a minimum required QoS rate defined by R_q, is formulated in (12) as:

$$q_i(\boldsymbol{\mu}, p_q) \geq R_q, \forall_q \tag{12}$$

In the subsequent formulations, $\frac{a_{1,q}}{\sigma^2}$ in (11) is denoted by $\bar{a}_{1,q}$. From (11), the sum of the amount of data bits that the WQS q in the group 2 could transmit can now be formulated in (13) as:

$$R_{sum}(\boldsymbol{\mu}, p_q) = \sum_{q=1}^{Q} r_q(\boldsymbol{\mu}, p_q), \forall_q \tag{13}$$

By combining (11) and (13), (14) is derived as:

$$R_{sum}(\boldsymbol{\mu}, p_q) = \beta W \log_2\left(\sum_{q=1}^{Q} \bar{a}_{1,q}\ p_q + 1\right),\ \forall_q \tag{14}$$

3.3. Power *consumption model*

The model of the power consumption of the new WPSN in the DL and in the UL stages is considered in this part. The consumed energy in the DL is defined as E_{DL}, and characterizes the sum of the total consumed energy by E_{DL1} and E_{DL2} for group 1 and group 2, respectively. It includes the cost for the DPSs circuit consumption for hardware processing and the transmission power. Hence, the total consumed energy in the DL by all the WQSs i in group 1 during EH can be modeled in (15) as:

$$\mathrm{E}_{DL1}(\tau, P_{A,g}) = \sum_{g=1}^{G}\left(P_{A,g} + P_c - \sum_{i=1}^{I} \eta\left(b_{g,i}\, P_{A,g}\right)\right)\tau, \quad \forall_i \in \{i_1,\ i_2, \dots,\ I\} \tag{15}$$

where P_c is the DPSs' circuit power. For practical purposes, the sum in (15) must be positive because of the law of energy conservation.

Also, the total energy consumption of all the WQSs q in group 2 in the DL is modeled in (16) as:

$$\mathrm{E}_{DL2}(\tau, P_{A,g}) = \sum_{g=1}^{G}\left(P_{A,g} + P_c - \sum_{q=1}^{Q} \eta\left(b_{g,q}\, P_{A,g}\right)\right)\tau, \quad \forall_q \in \{q_1,\ q_2, \dots,\ Q\} \tag{16}$$

Again, the sum must also be positive.

Therefore, the overall consumed energy by both groups 1 and 2 is modelled in (17) as:

$$\mathrm{E}_{DL}(\tau, P_{A,g}) = \sum_{g=1}^{G}\left(P_{A,g} + P_c - \sum_{i=1}^{I} \eta\left(b_{g,i}\, P_{A,g}\right) + \sum_{q=1}^{Q} \eta\left(b_{g,q}\, P_{A,g}\right)\right)\tau, \quad \forall_i \cup \forall_q \tag{17}$$

The energy consumed in the UL stage during information transmission in cycle one by group 1 is denoted by E_{UL1}, while E_{UL2} defines the energy consumed by group 2 at the UL stage. The scheduled WQSs i for data communication spend the harvested energy to communicate their individual signals to the sink node using resources p_i and β. Hence, the energy that each WQS i in group 1 spent is formulated in (18) as:

$$p_i + p_{i,c} \leq \frac{E_i}{\beta}, \forall_i \tag{18}$$

In (18), $p_{i,c}$ defines WQS i circuit power consumption Hence, the total energy that the group 1 WQSs i spent in the UL is modeled in (19) as:

$$\mathrm{E}_{UL1}(\beta, p_i) = \sum_{i=1}^{I}\left(p_i + p_{i,c}\right)\beta \tag{19}$$

Also, for the group 2 WQSs q, the energy spent by each WQS q can be formulated in (20) as:

$$p_q + p_{q,c} \leq \frac{E_q}{\beta}, \forall_q \tag{20}$$

Note that $p_{q,c}$ is the WQS q circuit power consumption.

Also, the total spent energy by the WQSs q in group 2 in the UL is modeled in (21) as:

$$\mathrm{E}_{UL2}(\beta, p_q) = \sum_{q=1}^{Q}\left(p_q + p_{q,c}\right)\beta \tag{21}$$

At this point, it is key to emphasize that the total energy that the new WPSN spent in cycle 1 is independent of E_{UL2}, therefore, by using (17) and (19), the total energy that the proposed system spent in cycle one is formulated in (22) as:

$$E_{tot1} = \mathrm{E}_{DL}(\tau, P_{A,g}) + \mathrm{E}_{UL1}(\beta, p_i) \tag{22}$$

$$E_{tot1} = \mathrm{E}_{DL}(\tau, P_{A,g}, \beta, p_i) = \sum_{g=1}^{G}\left(P_{A,g} + P_c - \sum_{i=1}^{I} \eta\left(b_{g,i}\, P_{A,g}\right) + \sum_{q=1}^{Q} \eta\left(b_{g,q}\, P_{A,g}\right)\right)\tau + \sum_{i=1}^{I}\left(p_i + p_{i,c}\right)\beta \tag{23}$$

Also, by using (17) and (21), the total energy that the new WPSN spent in cycle two is independent of E_{UL1}, and is expressed in (24) as:

$$E_{tot2} = \mathrm{E}_{DL}(\tau, P_{A,g}) + \mathrm{E}_{UL2}(\beta, p_q) \tag{24}$$

(24) implies that: $E_{tot2} = \mathrm{E}_{DL}(\tau, P_{A,g}, \beta, p_q) = \sum_{g=1}^{G}\left(P_{A,g} + P_c - \sum_{i=1}^{I} \eta\left(b_{g,i}\, P_{A,g}\right) + \sum_{q=1}^{Q} \eta\left(b_{g,q}\, P_{A,g}\right)\right)\tau + \sum_{q=1}^{Q}\left(p_q + p_{q,c}\right)\beta$ (25)

Due to the successive mode of operation of the proposed WPSN system, problems (23) and (25) holds independently such that (23) is enabled in cycle 1, while (25) operates in cycle 2.

4. Energy efficiency optimization problem

This part formulates the EE of the proposed WPSN system as an optimization problem to optimize the efficiency of the system. It is crucial to underline that EE is an essential metric in communication systems including WPSNs as it provides a platform for quantitatively measuring the data bits that are reliably transmitted at the transmitter to a receiver and the energy consumed. Note that the overall EE of a WPSN is affected by the number of WQM nodes present in the network, hence, the need for efficient resource allocation schemes for reducing the overall energy utilization so as to improve the EE of the system. Consequently, the EE of the new WPSN is maximized by determining the ratio of the system sum-data to the total energy consumption (bits/J). In this study, two EE optimization problems, P1 and P2, are formulated for the successive WQS nodes i and q in groups in 1 and 2, respectively. Based on (8) and (23), the EE of the system configured with the group 1 successive WQS nodes i in cycle one is formulated in Problem (26) with respect to constraints (27) - (32) as:

$$\text{P1:} \quad \max_{\boldsymbol{\mu},\ P_{A,g},\ p_i} \quad \frac{R_{sum}(\boldsymbol{\mu}, p_i)}{E_{tot1}} \tag{26}$$

subject to:

$$\tau + \beta \leq 1 \tag{27}$$
$$0 \leq P_{A,g} \leq P_{max} \tag{28}$$
$$\left(p_i + p_{i,c}\right)\beta \leq \eta \sum_{g=1}^{G} P_{A,g}\, b_{g,i}\tau + e_{i,}\ \forall_i \tag{29}$$
$$0 \leq p_i \leq \bar{p}_i,\ \forall_i \tag{30}$$
$$\tau \geq 0\,, \forall_g \cup \forall_i \tag{31}$$
$$\beta \geq 0\,,\ \forall_i \cup g_1 \tag{32}$$

P2 is formulated for the group 2 successive WQS nodes q in cycle two in (33) based on (14) and (25), and is subject to constraints (27), (28), (34) – (37) as follows:

$$\text{P2:} \quad \max_{\boldsymbol{\mu},\ P_{A,g},\ p_q} \quad \frac{R_{sum}(\boldsymbol{\mu}, p_q)}{E_{tot2}} \tag{33}$$

subject to:

(27), (28),

$$\left(p_q + p_{q,c}\right)\beta \leq \eta \sum_{g=1}^{G} P_{A,g}\, b_{g,q}\tau + e_q$$
$$\forall_q \in \{q_1,\ q_2, \dots,\ Q\} \tag{34}$$
$$0 \leq p_q \leq \bar{p}_q,\ \forall_q \in \{q_1,\ q_2, \dots,\ Q\} \tag{35}$$
$$\tau \geq 0\,, \forall_g \in \{g_1,\ g_2, \dots,\ G\} \cup$$
$$\forall_q \in \{q_1,\ q_2, \dots,\ Q\} \tag{36}$$
$$\beta \geq 0\,,\ \forall_q \in \{q_1,\ q_2, \dots,\ Q\} \cup g_1 \tag{37}$$

The EE optimization problems in (26) and (33) are non-convex and their convexity may be difficult to derive due to their fractional structures, thus, a nature inspired-based method is adopted to seek efficient solutions to the EE optimization problems.

5. Proposed solution

To obtain optimal solutions to (26) and (33), they are further simplified and a meta-heuristic-based method such as particle swarm optimization (PSO) is employed. The PSO algorithm is suitable for solving non-convex optimization problems because of its computational efficiency in the context of processing speed, fast convergence rate, and better solutions when compared to other methods such as genetic algorithm (GA) and ant-colony optimization (ACO) algorithm [26]. This is due to the lack of evolution operators in PSO [27], which consequently limits the number of its parameters compared to others.

Lemma 1: The power allocation problem for Problem (26) and (33) is solved for optimal EE when $P_{A,g}$ is set to P_{max}.

The proof of $P_{A,g} = P_{max}$ can be obtained in a similar manner as in [9] and [13], so that $P_{A,g} = P_{A,g}^*$, $p_i = p_i^*$, and $p_q = p_q^*$, and it is omitted here. Therefore (26) and (33) are rewritten in (38) and (39) as:

$$EE\ (\tau, \beta, p_i) = \frac{W\ log_2\left(\sum_{i=1}^{I} \bar{a}_{1,i}\, p_i + 1\right)}{\sum_{g=1}^{G}\left(\sum_{i=1}^{I} \eta b_{g,i}\, P_{max} + \sum_{q=1}^{Q} \eta b_{g,q}\, P_{max}\right)\frac{\tau}{\beta} + \sum_{q=1}^{Q}\left(p_i + p_{i,c}\right)} \tag{38}$$

$$EE\ (\tau, \beta, p_q) = \frac{W\ log_2\left(\sum_{q=1}^{Q} \bar{a}_{1,q}\, p_q + 1\right)}{\sum_{g=1}^{G}\left(\sum_{i=1}^{I} \eta b_{g,i}\, P_{max} + \sum_{q=1}^{Q} \eta b_{g,q}\, P_{max}\right)\frac{\tau}{\beta} + \sum_{q=1}^{Q}\left(p_q + p_{q,c}\right)} \tag{39}$$

Lemma 2: The EH duration allocation problem for (26) and (33) are solved for optimal EE when $\tau + \beta = 1$ [13].

Proof: Assume that the optimal time allocation $\tau^* + \beta^* < 1$ for (26) and (33) exists in solutions $\{\tau^*,\ P_{A,g}^*, p_i^*, \beta^*\}$ and $\{\tau^*,\ P_{A,g}^*, p_q^*, \beta^*\}$, then feasible points $\{\bar{\tau}^*,\ \bar{P}_{A,g}^*, \bar{p}_i^*, \bar{\beta}^*\}$ and $\{\bar{\tau}^*,\ \bar{P}_{A,g}^*, \bar{p}_q^*, \bar{\beta}^*\}$ could be constructed when $\bar{\tau} + \bar{\beta} = 1$, $\bar{P}_{A,g} = P_{A,g}^*$, $\bar{p}_i = p_i^*$, $\bar{p}_q = p_q^*$, as well as $\bar{\tau}/\bar{\beta} = \tau^*/\beta^*$. Considering the above scenarios, it is simple and straightforward to infer that the optimal time allocation for an optimal EE - denoted as EE^* - is achieved when $\tau + \beta = 1$ since $\overline{EE} = EE^*$ will always hold.

Based on Lemma 2, (26) and (33) are further reformulated by replacing τ with $1 - \beta$, as follows:

$$\max_{(\beta, p_i) \in \mathrm{R}_1 \times \mathrm{S}_1} \quad EE\left(\beta,\ p_i\right) = \frac{W\ log_2\left(\sum_{i=1}^{I} \bar{a}_{1,i}\, p_i + 1\right)}{\sum_{g=1}^{G}\left(\sum_{i=1}^{I} \eta b_{g,i}\, P_{max} + \sum_{q=1}^{Q} \eta b_{g,q}\, P_{max}\right)\left(\frac{1}{\beta} - 1\right) + \sum_{i=1}^{I}\left(p_i + p_{i,c}\right)} \tag{40}$$

$$\max_{(\beta, p_q) \in \mathrm{R}_2 \times \mathrm{S}_2} \quad EE\left(\beta,\ p_q\right) =$$

$$\frac{W\ log_2\left(\sum_{q=1}^{Q}\bar{a}_{1,q}\ p_q+1\right)}{\sum_{g=1}^{G}\left(\frac{P_{max}+P_c\ -}{\sum_{i=1}^{I}\eta b_{g,i}\ P_{max}+\sum_{q=1}^{Q}\eta b_{g,q}\ P_{max}}\right)\left(\frac{1}{\beta}-1\right)+\sum_{q=1}^{Q}(\ p_q+p_{q,c})} \quad (41)$$

subject to:

$$(p_i+p_{i,c})\beta \le \eta\sum_{g=1}^{G} P_{max}\ b_{g,i}(1-\ \beta)+\ e_i\ ,$$
$$\forall_i \in\ \{i_1,\ i_2,\dots,\ I\} \quad (42)$$

$$\beta W\ log_2\left(1+\frac{a_{1,i}\ p_i}{\sum_{d=i+1}^{I} a_{1,d}\ p_d+\sigma^2}\right) \ge R_i,$$
$$\forall_i \in\ \{i_1,\ i_2,\dots,\ I\} \quad (43)$$

$$(p_q+p_{q,c})\beta \le \eta\ \sum_{g=1}^{G} P_{max}\ b_{g,q}(1-\ \beta)+\ e_q\ ,$$
$$\forall_q \in \{q_1,\ q_2,\dots,\ Q\} \quad (44)$$

$$\beta W\ log_2\left(1+\frac{a_{1,q}\ p_q}{\sum_{d=q+1}^{Q} a_{1,d}\ p_d+\sigma^2}\right) \ge R_i,$$
$$\forall_q \in \{q_1,\ q_2,\dots,\ Q\} \quad (45)$$

Note that:

$$\mathrm{R}_1 = \{\beta |\ 0\ \le\ \beta\ \le 1\}$$
$$\mathrm{S}_1 = \left\{\begin{matrix}\{(\ p_1,\ p_2,\dots,\ p_I)|0\ \le\ p_i \le\ \bar{p}_i, \forall_i \in \\ \{i_1,\ i_2,\dots,\ I\}\end{matrix}\right\}$$
$$\mathrm{R}_2 = \{\beta |\ 0\ \le\ \beta\ \le 1\}$$
$$\mathrm{S}_2 = \left\{\begin{matrix}\{(\ p_1,\ p_2,\dots,\ p_Q)|0\ \le\ p_q \le\ \bar{p}_q, \forall_q \in \\ \{q_1,\ q_2,\dots,\ Q\}\end{matrix}\right\}$$

$\mathrm{R}_1 \times \mathrm{S}_1$ is used to denote the product of the Cartesian of R_1 and S_1, and $\mathrm{R}_2 \times \mathrm{S}_2$ defines the product of the Cartesian of R_2 and S_2.

Lemma 3: The optimal time and power allocation for (40) and (41) can be achieved by:

$$\beta = \min\left\{1,\ min\frac{\eta\sum_{g=1}^{G} P_{max}\ b_{g,i}+e_i}{\eta\sum_{g=1}^{G} P_{max}\ b_{g,i}+p_i\ +p_{i,c}}\right\},$$
$$\forall_i \in \{i_1,\ i_2,\dots,\ I\} \quad (46)$$

$$\beta = \min\left\{1,\ min\frac{\eta\sum_{g=1}^{G} P_{max}\ b_{g,q}+e_q}{\eta\sum_{g=1}^{G} P_{max}\ b_{g,q}+p_q\ +p_{q,c}}\right\},$$
$$\forall_q \in \{q_1,\ q_2,\dots,\ Q\} \quad (47)$$

Therefore, (46) and (47) satisfies the optimal(β, p_i), and (β, p_q), respectively.

In order to apply a PSO-based algorithm to (40) and (41), the problems are represented by EE(χ), and χ relies on variables (β, p_i) and (β, p_q) for groups 1 and 2, respectively. Also, each individual WQS i in group 1 is represented by a particle, and each i is a potential solution to (40). The position of each particle i is given by vector χ_i, and is represented using Cartesian coordinates (x, y). The vector form for the position expression of particles i which includes $(1 \le i \le C)\ \forall_i \in \{i_1,\ i_2,\dots,\ I\}$ is $\chi_i = \left[x_{i_1}\ x_{i_2}\dots x_{I_{\mathrm{F}}}\right]^T$, where C is the maximum number of particles, and $\mathrm{F} \in \{i_1,\ i_2,\dots,\ I\}$. Note that the position of each particle i includes variables for the transmission time and power allocation in the objective function (40), as well as the constraints in (42) and (43). χ_i has a time index which is given by $\chi_i(t)$. In addition to the position, each particle i has a velocity which is represented by $\upsilon_i(t)$. The $\upsilon_i(t)$ is a vector that indicates the movement of each particle i in terms of direction and distance. To determine the fitness value of i for EE($\chi_i(t)$) in each iteration, the position and the velocity of each particle i is updated according to the proposed energy-efficient PSO-based model (EEPSOM) given in Algorithm 1. Analogously, each individual WQS q in group 2 is denoted by a particle that serves as a potential solution to (41). Each particle q is defined by vector χ_q and represented by coordinates (x, y). The vector form for the position expression of particles q containing $(1 \le q \le E)\ \forall_q \in \{q_1,\ q_2,\dots,\ Q\}$ is $\chi_q = \left[x_{q_1}\ x_{q_2}\dots x_{Q_{\mathrm{H}}}\right]^T$, where E is the maximum number of particles, and $\mathrm{H} \in \{q_1,\ q_2,\dots,\ Q\}$. The position of each particle q includes the transmission time and power allocation variables in the objective function (41) and the constraints in (44) and (45). The time index and velocity of each particle q is defined by $\chi_q(t)$ and $\upsilon_i(t)$. The fitness value of q for EE($\chi_{iq}(t)$) in each iteration is updated based on the proposed energy-efficient PSO-based model (EEPSOM) in Algorithm 1. In Algorithm 1, c_1 and c_2 are used to denote the acceleration coefficients. In PSO, the standard value for each is 2. Also, ω is used to represent the initial coefficient which has a standard value of 1 [26], [24]. As already stated in the formulations, η is the energy conversion efficiency. In Algorithm 1, V_{max} is used to describe the maximum movement a particle can make during iterations, while *B* indicates the maximum iteration number.

Algorithm 1. EEPSOM

Require: c_1, c_2, η, ω, V_{max}, *C*, *B*, *E*

Solving for group 1 successive WQSs *i* EE in cycle one

for i = 1:*C* **do**
  set t = 0 to begin the algorithm
  generate feasible random particles $\chi_i(t)$ with a velocity of $\upsilon_i(t)$, such that $\upsilon_i(t)$ is bounded by a lower bound of $-V_{max}$ and an upper bound of V_{max}
  calculate particle $i's$ fitness value, EE($\chi_i(t)$), using the fitness function based on (40), (42), (43) and set particle $i's$ best solution as $\bar{\chi}_{iPbest}(t)$, up to the *i-th* iteration
  choose the particle that has the best fitness value among the particle $i's$ and set the best solution as $\bar{\chi}_{iGbest}(t)$, up to the *i-th* iteration
  repeat
end for
for each particle *i* **do**
  set t = t + 1
  calculate the particle velocity $\upsilon_i(t+1)$ as:
    $\upsilon_i(t+1) = \omega\ \upsilon_i(t) + \mathrm{c}_1\ \eta(\bar{\chi}_{iPbest}(t) - \chi_i(t)) + \mathrm{c}_2\ \eta(\bar{\chi}_{iGbest}(t) - \chi_i(t))$
  update the position of each particle using:
    $\chi_i(t+1) = \chi_i(t) + \upsilon_i(t+1)$
end for
for each particle *i* **do**
  if EE$(\chi_i(t)) \gg (\bar{\chi}_{iPbest}(t))$ **then**
    update $\bar{\chi}_{iPbest}(t) = \chi_i(t)$

16: **end if**
17: **if** EE$(\chi_i(t)) \gg (\bar{\chi}_{iGbest}(t))$ **then**
18: update $\bar{\chi}_{iGbest}(t) = \chi_i(t)$
19: **end if**
20: **end for**
21: repeat up until t is greater than B
22: return $\bar{\chi}_{iGbest}(t)$
23: until convergence

Solving for group 2 successive WQSs q EE in cycle two

24: **for** q = 1:E **do**
25: set t = 0 to begin the algorithm
26: generate feasible random particles $\chi_q(t)$ with a velocity of $\upsilon_q(t)$, such that $\upsilon_q(t)$ is bounded by a lower bound of -V_{max} and an upper bound of V_{max}
27: calculate particle $q's$ fitness value, EE($\chi_q(t)$) , using the fitness function based on (41), (44), (45) and set particle $q's$ best solution as $\bar{\chi}_{qPbest}(t)$, up to the *q-th* iteration
28: choose the particle that has the best fitness value among the particle $q's$ and set the best solution as $\bar{\chi}_{qGbest}(t)$, up to the *q-th* iteration
29: repeat
30: **end for**
31: **for** each particle q **do**
32: set t = t + 1
33: calculate the particle velocity $\upsilon_q(t+1)$ as:

$$\upsilon_q(t+1) = \omega\ \upsilon_q(t) + c_1\ \eta(\bar{\chi}_{qPbest}(t) - \chi_q(t)) + c_2\ \eta(\bar{\chi}_{qGbest}(t) - \chi_q(t))$$

34: update the position of each particle using:
$\chi_q(t+1) = \chi_q(t) + \upsilon_q(t+1)$
35: **end for**
36: **for** each particle i **do**
37: **if** EE$(\chi_q(t)) \gg (\bar{\chi}_{qPbest}(t))$ **then**
38: update $\bar{\chi}_{qPbest}(t) = \chi_q(t)$
39: **end if**
40: **if** EE$(\chi_q(t)) \gg (\bar{\chi}_{qGbest}(t))$ **then**
41: update $\bar{\chi}_{qGbest}(t) = \chi_q(t)$
42: **end if**
43: **end for**
44: repeat up until t is greater than B
45: return $\bar{\chi}_{qGbest}(t)$
46: **until** convergence

For the scheduling of group 1 and group 2 WQSs i and q for UL water quality data communication, a scheduling algorithm is implemented on the proposed WPSN system controller to enable either group 1 or group 2 in a cycle using a pre-defined scheduling priority. The scheduling algorithm is referred to as a successive scheduling algorithm for UL operation (SSAUL) and is presented in Algorithm 2.

Algorithm 2. SSAUL

1: **Initialize**: group1 $\triangleq \{i_1, i_2, \dots, I\}$
group2 $\triangleq \{q_1, q_2, \dots, Q\}$
group $\in \{1, 2\}$
groups $\in$ group1 $\cup$ group2
Maximum iteration group $\vartheta \in$ group2
2: **repeat**
3: **for** group = 1; group <= groups; group++ **do**
4: **if** group = = 1 **then**
5: **Initialize**: i = 0, schedule group1 in cycle one
6: **repeat**
7: set $i = i + 1$ to enable all i's in group1 to simultaneously transmit data to g_1
until $i \leq I$
8: return
9: **end if**
10: **else if** group = = 2 **then**
11: **Initialize**: q = 0, schedule group2 in cycle two
12: **repeat**
13: set $q = q + 1$ to enable all q's in group2 to simultaneously transmit data to g_1
14: **until** $q \leq Q$
15: return
16: **end if**
17: **end for**
18: **until** group < ϑ

The performance of the SSAUL algorithm has a complexity of $\mathcal{O}(group2)$, which indicates a linear complexity. This is an indication that the proposed scheduling complexity is tractable, low, and solvable in a linear time. The low complexity of the SSAUL algorithm is highly advantageous to the proposed system as it prevents the new system from being over-burdened.

6. Simulation results and discussion

The system is configured with the parameters in Table I to facilitate results comparison of the proposed successive WPSN system with a contemporary WPSN system [15].

Table 1 Simulation settings

Parameter	Setting	References
DPS maximum transmit power, P_{max}	10 W	[14],[15]
DPS circuit power, P_c	500 mW	[14],[15]
Operating frequency	2.4 GHz	[15]
Energy conversion efficiency, η	0.9 (ratio)	[15]
Sensor maximum transmit power, $\bar{p}_i = \bar{p}_q$	1 W	[13],[15]
Sensor circuit power, $p_{i,c} = p_{q,c}$	10 mW	[13],[15]
System bandwidth, W	20 kHz	[15]
Initial energy, $e_i = e_q$	0 J	[15]
Channel path loss exponent, φ	2	[8],[14],[15]
Noise power, σ^2	-110 dBm	[8],[14],[15]
Minimum required throughput, $R_i = R_q$	2 kbit/s	[15]

The formation of the new WPSN system is comprised of the group 1 WQSs i, group 2 WQS q, and the DPSs g, one of which is designated as the HPSSN. As in the reference WPSN system [15], the WQSs i and the WQSs q both have a reference distance in meter to g_1, and is defined as d_i (m) = d_q (m) = 2.5_i (m) = 2.5_q (m), $\forall_i \cup \forall_q$. Because of the DL and UL channel-links reciprocity, the channel-links are formed as $b_{g,i} = a_{g,i} = 10^{-1} d_{g,i}^{-\varphi}$ for $\forall_i$ in group 1, and $b_{g,q} = a_{g,q} = 10^{-1} d_{g,q}^{-\varphi}$ for $\forall_q$ in group 2. In the formulated channel model, φ stands for the path loss exponent and is set to 2, while $d_{g,i}$ and $d_{g,q}$ defines the between a DPS g and a WQS i and q in group 1 and group 2. The EEPSOM algorithm was implemented using the PSO-based model, and we define V_{max} to be 10^{-3}, and B to be 320.

6.1. *Performance comparison*

To investigate the efficiency of the proposed algorithm in terms of convergence, it was compared with two well-known meta-heuristic algorithms, namely GA and ACO. Also, for the purpose of validation, the new system was compared with the PSO work in [15]. The simulation parameters used are $R_i = R_q$

= 2 kbits, a 4-sensor WPSN system powered by an HPSSN, with i = 2 WQSs, q = 2 WQSs, and all i WQSs scheduled in the UL by the successive WPSN system using the SSAUL algorithm, and 4-sensor WPSN system with J = 4 sensors.

It is clearly observed from Fig. 2 that the EEPSOM algorithm outperforms other algorithms as it reaches its optimal solution quickly compared to the ACO and GA. The proposed EEPSOM algorithm achieved a significant increase in convergence iterations of 0.33% and 0.37% in comparison with the ACO and GA algorithms, respectively. This implies a substantial performance gain by the EEPSOM algorithm.

Secondly, it appears clear that the achievable EE of the new system in Fig. 2 is greater than the reference system using the EEPSOM algorithm, and the average difference between the system EE of the proposed and the existing systems is 6.32%. This indicates that the performance gain of the EEPSOM algorithm is highly significant. This obviously shows the efficiency of the proposed system, and the employed PSO method.

In addition, the proposed meta-heuristic-based resource allocation scheme was compared with another scheme presented in the work in [13] which is a non-meta-heuristic-based resource allocation scheme, but an iterative Dinkelbach algorithm. To achieve this, both systems were investigated using the same configuration settings, and the outcomes of the two systems as indicated in Fig. 2 revealed the optimal efficiency of the proposed solution in a NOMA-based WPSN system over the time-division-mode-switching based WPSN system. The optimal performance gain is technically due to the efficiency of the proposed algorithmic solutions as well as the NOMA protocol.

Moreover, to gain insight into the performance of the proposed system as a function of the initial energy, the proposed system's performance is investigated when an initial energy is available (or reserved) in the sensors' i and q in-built batteries from the previous transmission blocks. For this purpose, an initial energy of 0.02 J is assumed, and e_i and e_q are both set to 0.02 J. As illustrated in Fig. 2, the magenta solid line plot with a diamond legend reveals the optimal EE performance gains of the proposed system when $e_i = e_q = 0.02$ J [14]. Note that the increase in the achieved EE is due to the fact that the available initial energy technically provided a room for more data bits to be transmitted, making the proposed system with an initial energy to achieve better optimal performance compared to the proposed system without an initial energy from the previous transmission blocks (here with a gain of about 0.72%).

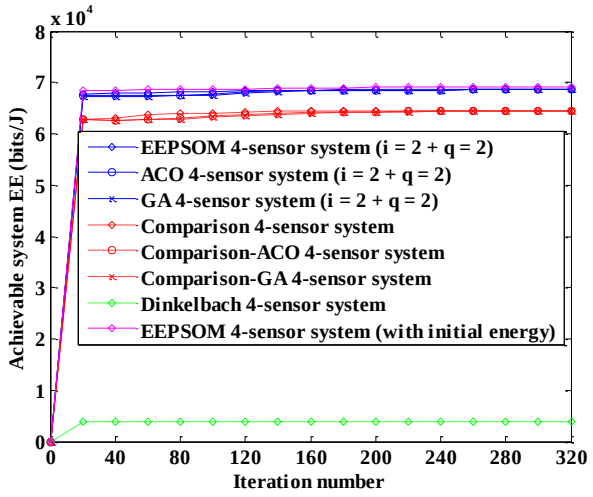

Fig. 2. Performance comparison of the proposed EEPSOM algorithm

6.2. *Impact of different data load on system EE*

This section investigated the effect of various data load to gain insights into the EE performance of the new system when the network is under a heavy load. Also, the new system is compared with the baseline work to further underline the contributions of the newly proposed solutions. For this reason, a configuration of 4-sensor WPSN system powered by an HPSSN, with i = 2 WQSs, q = 2 WQSs, and all i WQSs scheduled in the UL by the successive WPSN system using the SSAUL algorithm, and 4-sensor WPSN system with J = 4 sensors is considered as the data load is varied from $R_i = R_q$ = 2 kbits to $R_i = R_q$ = 16 kbits at an increment of 2 kbits. The outcomes of this investigation are described in Fig. 3.

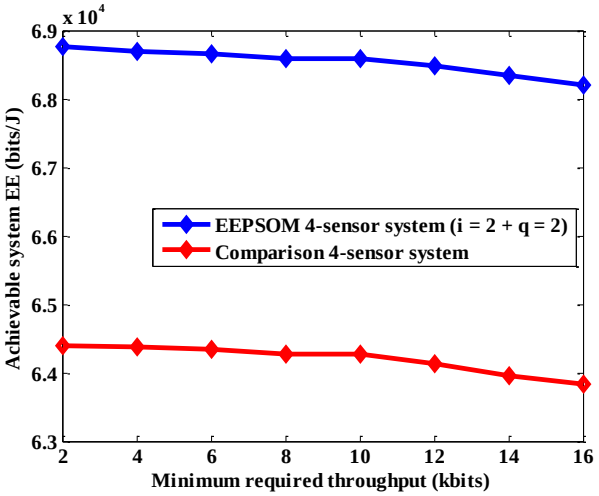

Fig. 3. Minimum required throughput versus system EE

From Fig. 3, the EE of the proposed system as well as the baseline system is observed to experience a slight decrease in performance when the network is under a light load for instance 2 kbits to 10 kbits, whereas the proposed system has a performance advantage of about 6.71%. Also, a significant decrease is observed under a heavy load, for example 10 kbits

beyond, as a result of higher minimum throughput QoS requirements to meet the demand of transmitting more data bits, but the proposed system maintains a performance advantage (6.56% at a load of 16 kbits). The comparison of the proposed solution and the baseline solution reveals that the newly proposed solution achieves a better performance with an overall gain of 6.64%, an indication of the efficiency of the proposed solution.

In the subsequent experiments, the P_{max} is set by the network manager to be 3W since it is more realistic and reasonable for WPSNs. For example, the existing DPS transmitters such as the Powercaster currently work at 1W to 3W, or the equivalent isotropic radiated power (EIRP). These are the acceptable transmission power levels in line with the regulations of the Federal Communications Commission. Although it is possible for the network nodes to harvest energy at higher power levels, the transmitters are not permitted by the current standards to transmit at higher power levels above 3W into air, so it is sensible to use this value as P_{max}.

6.3. *Performance analysis of group 1 and group 2 scheduling*

The section investigates the performance gains of group 1 and group 2 in cycle one and two respectively by varying the transmit power used to broadcast a continuous sinusoidal signal containing an RF energy by the DPS. For this reason, group 1 is configured as a 5-WQS WPSN containing i = 3 WQSs and q = 2 WQSs, both i and q WQSs are enabled in the DL, while only i WQSs are scheduled in the UL by the successive WPSN system in cycle one by employing the SSAUL algorithm. Also, group 2 is configured as a 5-WQS WPSN containing i = 3 WQSs and q = 2 WQSs, both i and q WQSs are enabled for EH in the DL, while only q WQSs are scheduled in the UL by the successive WPSN system using the SSAUL algorithm in cycle two. Both group 1 and group 2 i and q WQSs are powered by an HPSSN $\in$ {1W, 2W, 3W} transmission power. The performance comparison results are presented in Fig. 4.

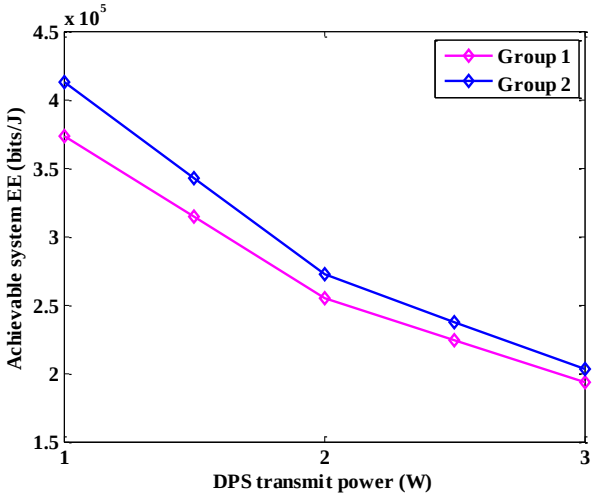

Fig. 4. Performance analysis of group 1 and group 2

From Fig. 4, it is noticeable that the performance gains of the system EE for both group 1 and group 2 significantly decreases as the transmit power of the HPSSN is increased from 1W to 3W. This is due to the fact that increase in the transmit power simultaneously increases the level of the energy consumption for WET because of the wireless channel propagation. This phenomenon reveals that large transmit power increases energy consumption in the DL during energy transfer, and reduces the EE performance of the system. Also, the two configurations were compared and it was observed that group 2 with fewer WQSs in the UL achieved a better system EE compared to the group 1 with a high number of i WQSs in the UL. This reveals that the incremental increase of the number of WQSs scheduled for data communication in the UL contributes to the overall energy consumption, and consequently impacts the EE performance of the system.

6.4. *Effect of circuit power consumption and transmit power*

An investigation into the impact of circuit power consumption and transmit power on the system EE performance is carried out for a 5-node WPSN containing i = 3 WQSs, q = 2 WQSs in the DL, i = 3 WQSs in the UL in cycle one for group 1, and containing i = 3 WQSs, q = 2 WQSs in the DL, q = 2 WQSs in the UL in cycle two for group 2. Both systems are powered by an HPSSN $\in$ {3W} transmission power. In each experiment, during cycle one and two, the circuit power consumption of WQSs i and q is fixed, while the transmit power of i and q WQSs for transmitting their individual signals is varied. The outcomes of the investigation are described in Fig. 5.

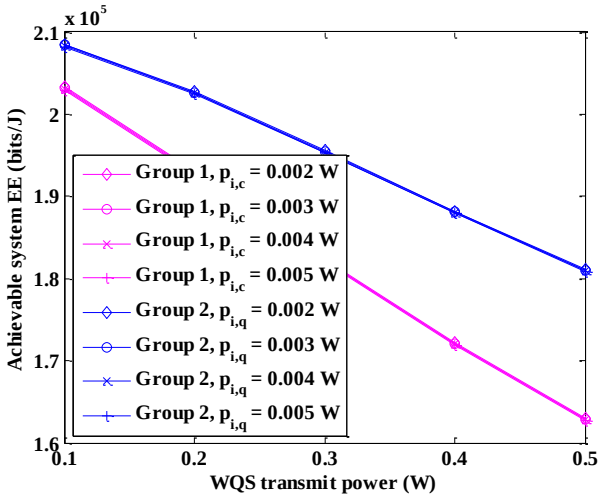

Fig. 5. Effect of circuit power consumption and transmit power

It is noticeable from Fig. 5 that the incremental of the WQSs i transmit power against a fixed value of the WQSs i circuit power consumption reveals a trade-off between the system EE, total energy consumption, and the sum-throughput such that increasing the transmit power of WQSs i increases the overall energy consumption of WQSs i during data communication in the UL in cycle one for group 1, decreases the system EE, and increases the sum-throughput. The main reason for the decrease

in the system EE is because of the overall increase in the total energy consumption. Also, the same decrease in the system EE in cycle one was also encountered in cycle two for group 2 as the transmit power of WQSs q increases over a fixed value of the WQSs q circuit power consumption. This is due to the similarities in the wireless channel conditions of WQSs i and q. Thus, for both successive group 1 and group 2, lower transmit power of WQSs i and q decreases the achievable throughput. It was also observed that the WPSN system scheduled for cycle two had an improved system EE performance gain compared to the one scheduled for cycle one. The improved EE result for cycle two could be attributed to number of q WQSs scheduled by the system in the UL.

6.5. *Impact of multiple DPSs on system EE*

The impact of multiple DPSs on the EE performance of the proposed system is studied in this section for two configurations including a 5-WQS WPSN containing i = 3 WQSs, q = 2 WQSs in the DL, WQSs i scheduled in the UL in cycle one for group 1, and a 5-WQS WPSN containing i = 3 WQSs, q = 2 WQSs in the DL, WQSs q scheduled in the UL in cycle two for group 2. These successive WPSN systems are powered by multiple DPSs by varying the number of the allocated DPS from one to three. Note that the P_{max} of the DPS is equal to 3W The outcomes of this investigation are described in Fig. 6.

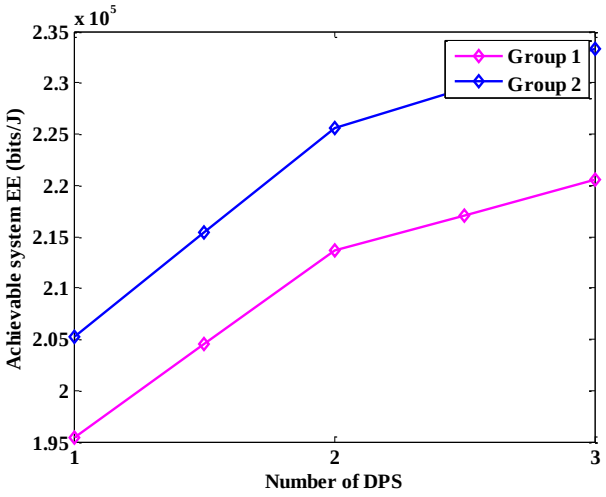

Fig. 6. Number of DPS versus system EE

From Fig. 6, it is evident that the performance of the system EE increases as the number of the allocated DPS is increased. This is because more DPSs in the DL causes lower energy loss because of good wireless channel states, and this consequently reduced the total energy consumption of the system. Also, with more DPSs, more energy can be harvested by the WQSs i and q over a short duration, and also the exploitation of more DPSs as well technically addressed the inherent fundamental doubly-near-far issue in WPSNs as the harvested energy fairness rate among WQSs i and q scheduled for EH in the DL is increased compared to the case of a single DPS that mostly suffers from poor wireless channel conditions. Furthermore, since the WQSs are able to harvest more energy in the case of multiple DPSs then large data bits can be supported in the UL. Note that more DPSs in the context of the considered scenario reveals a trade-off between EE and total energy consumption as the incremental of DPS increases the system EE performance gain in the two cycles and reduces the energy expenditure of the DL operations.

7. Conclusion

This study has dealt with the energy scarcity issue and as well enhanced the energy efficiency of a successive WPSN system devoted to WQM. Based on the proposed method, the new WPSN system reveals interesting simulation results. For example, the proposed EEPSOM algorithm outperforms the state-of-the-art contemporary meta-heuristic-based system in [15] and a non-meta-heuristic-based system in [13] when compared for a 4-WPSN system. The proposed successive WPSN system achieved encouraging energy utilization results.

It is key to emphasise that this study has provided a context for further interesting research problem such as the investigation of the energy efficiency performance of a NOMA-based WPSN system when there is a need to perform an operation like re-routing since such an operation may impact the EE energy performance of the system and is also expensive in the context of time and energy costs.

Acknowledgement

The authors would like to thank the editors and the anonymous reviewers for their suggestions which have greatly contributed to improving the quality of this paper.

References

[1] Editorial, "Water and sanitation: addressing inequalities", *The Lancet*, vol. 383, pp. 1359, Apr. 19, 2014.

[2] S.O. Olatinwo and T.H. Joubert, "Enabling communication networks for water quality monitoring applications: a survey," *IEEE Access*, vol. 7, pp. 100332-100362, Aug. 2019.

[3] S.O. Olatinwo and T.H. Joubert, "Energy efficient solutions in wireless sensor systems for water quality monitoring: a review", *IEEE Sensors Journal*, vol. 19, no. 5, pp. 1596-1625, Mar. 2019.

[4] S.O. Olatinwo and T.H. Joubert, "Efficient energy resource utilization in a wireless sensor system for monitoring water quality", *EURASIP Journal on Wireless Communications and Networking*, https://doi.org/10.1186/s13638-018-1316-x.

[5] Z. Sheng *et al.*, "A survey on the IETF protocol suite for the Internet of Things: standards, challenges, and opportunities," *IEEE Wireless Communications*, vol. 20, no. 6, pp. 91–98, Dec. 2013.

[6] P. Kamalinejad *et al.*, "Wireless energy harvesting for the Internet of Things," *IEEE Communications Magazine*, vol. 53, no. 6, pp. 102–108, Jun. 2015.

[7] M. R. Palattella *et al.*, "Internet of Things in the 5G era: enablers, architecture, and business models," *IEEE Journal on Selected Areas in Communications*, vol. 34, no. 3, pp. 510–527, Mar. 2016.
[8] S.O. Olatinwo and T.H. Joubert, "Optimizing the energy and throughput of a water-quality monitoring system", *Sensors*, vol. 18, no. 4, pp. 1-21, Apr. 2018.
[9] K. Chi, Y.H. Zhu, and Y. Li, "Efficient data collection in wireless powered communication networks with node throughput demands", *Computer Communications*, vol. 126, pp. 1-10, 2018.
[10] S. Guo, Y. Shi, Y. Yang, and B. Xiao, "Energy efficiency maximization in mobile wireless energy harvesting sensor networks", *IEEE Transaction on Mobile Computing*, vol. 17, no. 7, pp. 1524-1537, Jul. 2018.
[11] H. Yu, Y. Zhang, S. Guo, Y. Yang, and L. Ji, "Energy efficiency maximization for WSNs with simultaneous wireless information and power transfer", *Sensors*, vol. 17, no. 8, pp. 1-29, Aug. 2017.
[12] O. Amjad, E. Bedeer, and S. Ikki, "Energy efficiency maximization of self-sustained wireless body area networks", *IEEE Sensor Letters*, vol. 3, no. 12, Dec. 2019.
[13] X. Lin, L. Huang, C. Guo, P. Zhang, M. Huang, and J. Zhang, "Energy-efficient resource allocation in TDMS based wireless powered communication networks", *IEEE Communications Letters*, vol. 21, no. 4, pp. 861-864, Apr. 2017.
[14] Q. Wu, W. Chen and J. Li, "Wireless powered communications with initial energy: QoS guaranteed energy-efficient resource allocation," *IEEE Communication Letter*, vol. 19, no. 12, pp. 2278–2281, Dec. 2015.
[15] M. Song, and M. Zheng, "Energy efficiency optimization for wireless powered sensor networks with nonorthogonal multiple access", *IEEE Sensors Letters*, vol. 2, no. 1, Jan. 2018.
[16] K. Higuchi and A. Benjebbour, "Non-orthogonal multiple access (NOMA) with successive interference cancellation for future radio access," *IEICE Transactions on Communications*, vol. E98-B, no. 3, pp. 403–414, March 2015.
[17] Z. Ding *et al.*, "On the performance of non-orthogonal multiple access in 5G systems with random deployed users," *IEEE Signal Processing Letters*, vol. 21, no. 12, pp. 1501–1505, Dec. 2014.
[18] Z. Ding, M. Peng, and H.V. Poor, "Cooperative non-orthogonal multiple access in 5G systems," *IEEE Communications Letters*, vol. 19, no. 8, pp. 1462–1465, Aug. 2015.
[19] E. Balevi, F.T. Al Rabee, and R.D. Gitlin, "ALOHA-NOMA for massive machine-to-machine IoT communication" *in Proc. of the IEEE International Conf. Communications (ICC)*, Kansas City, USA, May 2018, pp. 1-5
[20] J.C. Kwan and A.O. Fapojuwo, "Radio frequency energy harvesting and data rate optimization in wireless information and power transfer sensor networks", *IEEE Sensors Journal*, vol. 17, no. 15, pp. 4862-4874, Aug. 2017.
[21] H. Ju and R. Zhang, "Throughput maximization in wireless powered communication networks", *IEEE Transactions on Wireless Communications*, vol. 13, no. 1, pp. 418-428, Jan. 2014.
[22] D. Mishra, S. De, and K.R. Chowdhury, "Charging time characterization for wireless RF energy transfer", *IEEE Transactions on Circuits and Systems-II: Express Briefs*, vol. 62, no. 4, pp. 362-366, Apr. 2015.
[23] Q. Wu, M. Tao, D.W.K. Ng, W. Chen, and R. Schober, "Energy-efficient resource allocation for wireless powered communication networks", *IEEE Transactions on Wireless Communications*, vol. 15, no. 3, pp. 2312-2327, Mar. 2016.
[24] K. Huang and E. Larsson, "Simultaneous information and power transfer for broadband wireless systems", *IEEE Transactions on Signal Processing*, vol. 61, no. 23, pp. 5972-5986, Dec. 2013.
[25] M. Carminati, V. Stefanelli, M. Sampietro, A. Turolla, M. Rossi, S. Malavasi, M. Antonelli, V. Pifferi, and L. Falciola, "Smart pipe: a miniaturized sensor platform for real-time monitoring of drinking water quality", *in Proc. of the IEEE Workshop on Environmental, Energy, and Structural Monitoring Systems (EESMS)*, Milan, Italy, Jul. 2017, pp. 1-6.
[26] E. Elbeltagia, T. Hegazy and D. Grierson, "Comparison among five evolutionary-based optimization algorithms", *Advanced Engineering Informatics*, vol. 19, no. 1, pp. 43-53, Jan. 2005.
[27] F. Marini and B. Walczak, "Particle swarm optimization (PSO). A tutorial", *Chemometrics and Intelligent Laboratory Systems*, vol. 149, pp. 153-165, 2015.

Segun O. Olatinwo received the B.Sc. (Hons.) and M.Sc. degrees in computer science and engineering. He is currently a research scholar at the University of Pretoria, South Africa. He is a registered member of engineering bodies. His research interests include energy efficient communications in wireless sensor networks and internet-of-things for water quality monitoring applications, energy harvesting, optimization and game theory, wireless powered networks, resource allocation, wireless communication systems, and half duplex and full duplex communications.

Trudi-H. Joubert received both the B.Eng and M.Eng degrees in electronic engineering with distinction, and earned a Ph.D in electronic engineering from the University of Pretoria, South Africa, in 1996.

From 1987 to 2000, she advanced from Lecturer to Assistant Professor at the University of Pretoria. Between 2001 and 2013, she consulted to the microelectronics industry though Solid State Technology. She has worked on 31 projects for the South African industry, writing 129 technical reports in the process, and contributing to 32 integrated circuit chips. In 2013-4, she worked as senior

research engineer at the Council for Scientific and Industrial Research, South Africa, before returning to the University of Pretoria since 2015. Her core pursuit is CMOS and BiCMOS mixed signal circuit design, mainly in readout and signal processing for imaging arrays, biologically inspired electronic circuit applications, and specialized devices for analog IC design. Her most recent endeavour is printed electronics biosensors and networks, particularly for water quality monitoring. She has published 21 journal papers, and presented and co-authored 55 conference proceedings papers.

She is registered as a professional engineer with the Engineering Council of South Africa (ECSA), became a Member (M) of IEEE in 1996, and a Senior Member (SM) in 2015.